PROCEEDINGS OF SCIENCE

A novel method to search for point sources of ultra-high energy neutral particles using spacetime information

Miguel Alexandre Martins,[a,b,*] **Lorenzo Cazon,**[a] **Ruben Conceição,**[b] **Jaime Alvarez-Muñiz**[a] **and Enrique Zas**[a]

[a] *Instituto Galego de Física de Altas Enerxías,*
Rúa de Xoaquín Díaz de Rábago, s/n, Campus Vida, Universidade de Santiago de Compostela 15705 Santiago de Compostela, Galicia, Spain

[b] *Laboratório de Instrumentação e Física Experimental de Partículas,*
Av. Prof. Gama Pinto, n.2, 1649-003 Lisboa, Portugal

E-mail: miguelalexandre.jesusdasilva@usc.es

We propose a new observable sensitive to small-scale anisotropies both in the arrival directions and the arrival times of cosmic ray events, to search for flares of high energy neutral particles, with a time scale ∼ 1 day, and moderate intensity.

Coherent periodic or explosive emissions of neutral particles induce, not only local spatial excesses of events with respect to an isotropic background of charged cosmic rays but also clusters of arrival times. However, traditional time-integrated blind and targeted searches disregard deviations from anisotropies in the time domain.

We show that by adding information on the arrival time distribution of events in angular windows of the order of the detector resolution of comic-ray experiments, we boost the sensitivity to flare events, increasing the significance of a detection, compared to time-integrated searches. Furthermore, we develop an end-to-end analysis for a novel observable and show how it can be used in both blind and targeted searches, thus demonstrating its versatility and wide range of applicability.

38th International Cosmic Ray Conference (ICRC2023)
26 July - 3 August, 2023
Nagoya, Japan

*Speaker

PoS(ICRC2023)451

1. Introduction

In ultra-high energy cosmic ray experiments, such as the Pierre Auger Observatory (PAO) [1] and Telescope Array (TA) [2, 3], searches for neutral particles, such as photons, astrophysical neutrinos and neutrons, either rely on the analysis of shower observables that distinguish photonic or neutrino showers from hadronic ones [4–7] or on discerning local excesses of events in the sky from an isotropic cosmic ray background, either blindly [8] or in correlation with target sources [9]. The latter searches are time-integrated, although in neutrino experiments such as IceCube [10], time dependent searches for multi-flares of neutrinos have been published [11] with the method presented in [12]. Unlike cosmic rays, which are deflected by homogenous and random components of galactic and extra-galactic magnetic fields during their propagation from source to Earth, neutral particles emitted coherently at the source, keep their spatial and temporal coherence during propagation. Thus, disregarding the time coherence in time-integrated searches, might hamper the detection of fluxes from point sources of neutral particles, and, in particular, from flare events. A comprehensive list of candidate sources of photons and neutrons can be found in [13].

In this contribution, we develop a new observable sensitive to deviations from anisotropy in both the spatial and time domains. We build the probability density function of this observable for an isotropic background and perform blind and targeted searches for flares in mock datasets. We show that including the distribution of the arrival times of events boosts the sensitivity to flare events, motivating the application of the developed method to data to place stronger limits on the flux of neutral particles at ultra-high energies, or to increase the significance of a detection.

2. Analysis

2.1 Outline of time-integrated analysis

Blind time-integrated searches for small and intermediate scale anisotropies consist in defining target regions in the celestial sky, spanning a solid angle Ω_{target}, and counting the number of events in each target, n, to determine the probability of measuring at least n when μ are expected. Commonly, it is assumed that n follows a either a Poisson [9] or a binomial distribution [14], under the null hypothesis that the spatial distribution of events is spatially isotropic, irrespective of the distribution of arrival times. The collection of obtained *pre-trial* p-values is compared with the distribution of p-values obtained with an ensemble of samples of isotropically distributed events, by computing *pos-trial* p-values: the fraction of isotropic samples for which a p-values are less than or equal to the one observes for data [14].

In targeted searches, the procedure is similar, except that the targets are centered at the coordinates of candidate sources. In this case, assuming that the distribution of p-values is uniform, the penalized p-values for each target, for N_{targets} targets, are obtained via $p^* = 1 - (1 - p)^{N_{\text{targets}}}$ [9].

However, the aforementioned analysis overlook the requirement of a uniform distribution of arrival times of cosmic rays, even though it is expected from an isotropic flux of cosmic rays. Moreover, adding another constraint to the null hypothesis could boost the sensitivity to deviations from isotropy expectations.

2.2 Defining an estimator sensitive to spacetime anisotropies

To include information pertaining to the distribution of arrival times, we combine, for each target centered at $\mathbf{n}$, with n events, the $n-1$ time differences between consecutive events, Δt_i with $i \in \{1, 2, \ldots, n-1\}$, to define the quantity

$$\Lambda \equiv -\sum_{i=1}^{n-1} \ln\left(\Delta t_i \Gamma(\mathbf{n})\right), \tag{1}$$

where $\Gamma(\mathbf{n}) = \frac{\mu(\mathbf{n})}{T_{\text{obs}}}$ is the expected rate of events in a given target, for μ expected events and an observation time T_{obs}. This quantity is both sensitive to excesses of the number of events and to smaller time differences, whether they arise naturally from the event excess or by their clustering in time due to the presence of a flare. In both cases, larger values of Λ correspond to the clustering of events in space and time.

2.2.1 Parametrising distribution of Λ

To use Λ, which generalises the measured number of events n in a target, we have to determine its probability density function. To do so, 10^3 samples of isotropic distributions of 10^5 events are simulated[1]. These samples are obtained through a thorough scrambling procedure from a seed isotropic sample.

To generate the seed isotropic sample, we suppose an observatory at the location of PAO: average latitude of 35.15° S, longitude of 69.20 W, and height 1 400 m above sea level [1], and sample independently values of right ascension and declination, α_i and δ_i, uniformly distributed on a sphere. These correspond to the local zenith and azimuth angles, θ_i and ϕ_i. The arrival times of events are sampled from a uniform distribution over a time period of $T_{\text{obs}} = 10$ years, to match the exposures of PAO and TA. We either accept or reject each event by imposing $\theta_i < \theta_{\text{max}} = 80°$ in the instantaneous field of view[2] of the observatory for a given sidereal time $\alpha_0(t)$, and that the acceptance is suppressed by $\cos\theta$[3]. Note that the zenith angle cut-off defines the maximum declination $\delta_{\text{max}} = \theta_{\text{max}} + \ell_0 \sim 45°$, where ℓ_0 is the latitude of the observatory. In this simplified case, the instantaneous directional exposure, $\omega(\mathbf{n}, t) = \omega(\alpha, \delta, t)$ reads

$$\omega(\alpha, \delta, t) = C\left[\cos\ell_0 \cos\delta \cos(\alpha_0(t) - \alpha) + \sin\ell_0 \sin\delta\right] \quad \text{with } \theta(t, \alpha, \delta) < \theta_{\text{max}}, \tag{2}$$

where the constant C is such that $\iint \omega(\mathbf{n}, t)\, \mathrm{d}t\, \mathrm{d}\Omega = 1$. The formula for the time-integrated directional exposure, $\omega(\mathbf{n})$ is the one presented in [16], and it is only a function of the declination within our approximations, $\omega(\mathbf{n}) = \omega(\delta)$. Note further that, if N_{events} designates the total number of events, then

$$\mu = N_{\text{events}} \iint_{\Omega_{\text{target}}} \omega(\mathbf{n})\, \mathrm{d}\Omega = N_{\text{events}} \Sigma_{\text{target}}(\mathbf{n}) = N_{\text{events}} \Sigma_{\text{target}}(\delta), \tag{3}$$

where $\Sigma_{\text{target}}(\delta)$ is the integrated directional exposure over each target.

[1] Using the cosmic ray spectrum measured by the PAO [15], this corresponds to roughly all events $E_0 > 4$ eV, for a maximum zenith angle $\theta_{\text{max}} = 80°$, and over 10 years.

[2] Inclined showers above $\theta > 80°$ cannot be reliably reconstructed.

[3] This is the case for a flat horizontal array with constant area of the observation time.

The aforementioned scrambling procedure is performed by independently shuffling the arrival times t_i and zenith angles θ_i of the 10^5 events, and selecting ϕ_i uniformly from $[0, 2\pi]$. For each combination of t_i, θ_i and ϕ_i, the corresponding values of α_i and δ_i can be calculated. The procedure leaves the distributions of arrival times and zenith angles unchanged. For each sample of an isotropic sky, a circular target is defined around each event with a radius $\psi_{\text{target}} = 1^\circ$ (of the order of the angular resolution of the PAO [17]). The number of events, n, and the value of Λ, provided that there are at least two events in the target.

Assuming that the number of events in each target follows a Poisson, the time difference between consecutive events follows, to first approximation, an exponential distribution[4] with rate $\Gamma(\delta)$. Hence, the random variable $\tau = \ln(\Delta t \Gamma(\delta))$ follows the distribution $f_\tau(\tau) = \exp\{\tau - e^\tau\}$, and so, $\Lambda = -\sum_{i=1}^{n-1} \tau_i$ follows the $n-1$ self convolution, $f_\Lambda(\Lambda) = f_{\tau_1}(\tau_1) \circledast \cdots \circledast f_{\tau_{n-1}}(\tau_{n-1})$, which, as far as we know, cannot be performed analytically. Therefore, we parameterize this distribution in bins of $\Gamma(\delta)$, ranging from $\Gamma = 19$ to $\Gamma = 1$ events per decade. The lower limit of $\Gamma > 1$ eliminates some bias in the region with few events. For each bin of the expected event rate, the distribution of Λ is produced, and its upper tail fitted to an exponential function of the form $y = Ae^{-\beta\Lambda}$, where $\beta = \beta(\Gamma)$, by minimising χ^2. Only the upper tail needs to be fitted since high values of Λ reflect excesses of events in space and/or a clustering of events in time. The starting point of the fit range is chosen iteratively, starting at the 99% percentile of the Λ distribution and until the value of $\chi^2 < 2$. We have checked that the fit converges in each iteration and that the final fit range is representative of the extension of the tail of the Λ distribution.

The left panel of Figure 1 shows $f_\Lambda(\Lambda)$, for a few chosen bins of Γ, while the right panel displays the evolution of the exponential slope β as a function of the rate Γ. The color gradient is such that lower rates are represented in blue and high rates in red. The maximum expected rate is $\Gamma = 18$ decade^{-1}.

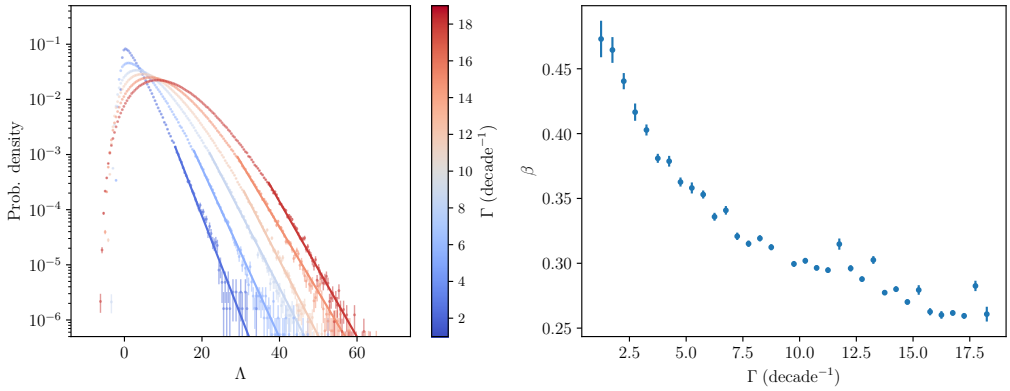

Figure 1: Left panel: distribution of Λ for bins in expected event rate, Γ, such that higher rates are represented in red and lower rates in blue, for 10^3 samples with 10^5 events isotropically distributed over 10 years, along with χ^2 fits to exponential functions. Right panel: exponential slope β of the upper tail of the Λ distribution as a function of the expected event rate.

It is apparent that the higher the expected rate, the flatter the tail of the distribution of Λ since

[4] This is only true to first order because the time difference is modulated by the rotation of the Earth and the observation time if finite, although much larger than the typical time differences between events.

more terms, with a larger value, are being added to the sum that defines this estimator (see Eq. 1). This tendency is clear from β as a function of the event rate.

To compute p-values of Λ for a target in a given expected rate band, its distribution is interpolated using a third-order Akima spline [18] and extrapolated using the exponential fit to the upper tail. The cumulative distribution of Λ, $F_\Lambda(\Lambda)$, is then built from the interpolated and extrapolated values of $f_\Lambda(\Lambda)$ to ensure its continuity.

3. Method

3.1 Obtaining sky samples with flares

To test the sensitivity of Λ to flare events, a catalogue of 1000 flares disturbed isotropically in the sky and uniformly in time is produced. Samples of skies with n_{flares} and n_{events} events per flare, each with the same duration ΔT_{flare}, are generated by sampling n_{events} events from each flare following a Gaussian distribution in the equatorial coordinates, centered at the position of the flare, and with width of 1°, and with arrival times sampled uniformly from the interval $[t_{\text{f}}, t_{\text{f}} + \Delta t_{\text{flare}}]$, where t_{flare} is the flare's time stamp. Afterwards, $n_{\text{events}} \times n_{\text{flares}}$ events are randomly removed from the isotropic sky and substituted with flare events.

3.2 Blind search

To perform a blind search for small-scale spacetime anisotropies, samples of skies with flares are binned using Healpix [19], with $n_{\text{side}} = 64$, corresponding to angular resolution of $\sim 1°$, to define the centers of each target, with $\psi_{\text{target}} = 1°$. The number of events, n, and the value of Λ are computed for each target, along with the corresponding p-values. For n, the p-value follows from a Poisson distribution via $p_{\text{poisson}} = 1 - \frac{1}{2}\left[\sum_{i=0}^{n-1} \text{Poisson}(i,\mu) + \sum_{i=0}^{n} \text{Poisson}(i,\mu)\right]$, where the averaging of cumulative distributions eliminates the bias towards lower or higher p-values. The p_Λ-value is computed from $p_\Lambda = 1 - F_\Lambda(\Lambda)$. This procedure is followed for the 10^3 samples of isotropic skies and a sample with flare events. From these, the corresponding *pos-trial* p-values are computed according to Section 2.1.

3.3 Targeted search

For the targeted search, we center each target at the position of each flares, computing and penalizing p-values for both n and Λ as described in 2.1. Note that the search in time is blind, although a targeted search could be addressed in the publication following this work.

4. Results

4.1 Blind search

Figure 2 shows the distributions of *pos-trial* p-values over the entire sky for the Poisson (left panel), and Λ (right panel) distributions, both with $n_{\text{flares}} = 20$ and $n_{\text{events}} = 5$ for each flare and two types of flares: short flares, with $\Delta t_{\text{flare}} = 1$ day, in red, and long flares, with $\Delta t_{\text{flare}} = 7$ days, represented in orange. Note the coordinates with the sources are kept constant between the two samples of short and long flares. The blue shaded areas represent 95% of the samples.

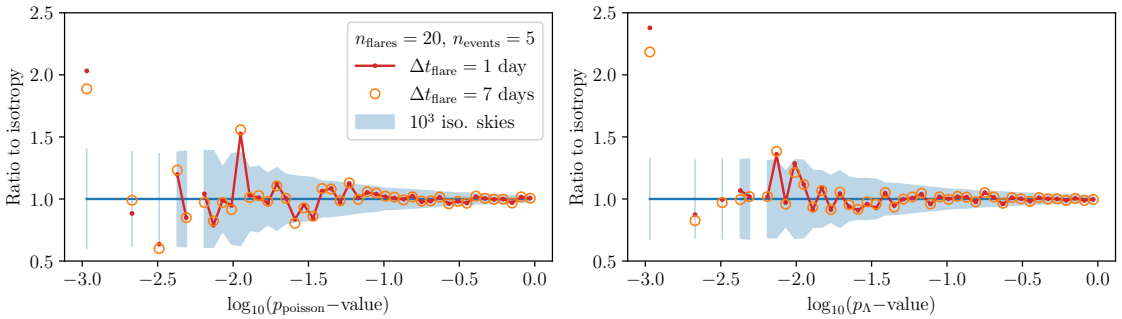

Figure 2: Left panel: distributions of p-values computed from the number of events in each target, as obtained for a sample with 20 flares and 5 events per flare, over $\Delta t_{\text{flare}} = 1$ day (short flare) in red, and $\Delta t_{\text{flare}} = 7$ days (long flare), in orange, normalized to a uniform distribution expected from isotropy. The blue bands correspond to 95% of the simulated isotropic samples. Right panel: the same as the left panel, but p-values are computed from Λ in each target.

The enhanced accumulation of points near $p-\text{value} = 10^{-3}$ for Λ, as compared to n, shows that Λ is more sensitive to the presence of small-scale spacetime anisotropies than a time-integrated estimator, thus rendering Λ more suited to search for flares of neutral particles. In particular, we observe a migration of events from p-value = 10^{-2} to p-value = 10^{-3}, hence an order of magnitude, by adding time information, irrespective of whether flares are shorter or longer. For longer flares, the sensitivity of Λ decreased, despite staying better than that provided by n. In an upcoming publication, the number of isotropic samples should be increased by an order of magnitude, to probe better lower p-values. A more systematic study of the dependence of the significance as a function of the flare duration will also be performed.

4.2 Targeted search

The penalised p-values for short and long flares are displayed in Figure 3, for short flares in the upper panel, and long flares in the lower panel. The left sky-maps refer to penalised p-values computed using the number of events in each target, the middle sky-maps refer to penalised p-values computed using Λ, and right histograms show the distribution of penalised p-values over the entire sky. In sky maps the colour scale is such that lower p-values are depicted in red and higher ones in blue. The blue dashed histograms pertain to p-values computed with n, red histograms to p-values computed with Λ for short flares, with $\Delta t_{\text{flare}} = 1$ day, and orange histograms to long flares, $\Delta t_{\text{flare}} = 7$ days.

Irrespective of the duration of the flare, the addition of time information yields lower penalized p-values, in same cases lower by an order of magnitude, as is clear from the distribution of penalized p-values, thus showing that Λ is far more sensitive than n to events coming from flares. In particular, for the set of short flares, 75% of the p-values for a time-integrated search are above 0.8, with the lowest p-value being 0.17, while the time-dependent search has 25% of the targets with p-value < 0.1, with the lowest reading 0.01. Results for longer flares are still very encouraging, despite the significance of the time-sensitive search being, on average, lower. Even so, 20% of the targets have a penalized p-value $< 1\%$, while the time-integrated search has none. Additionally, we note

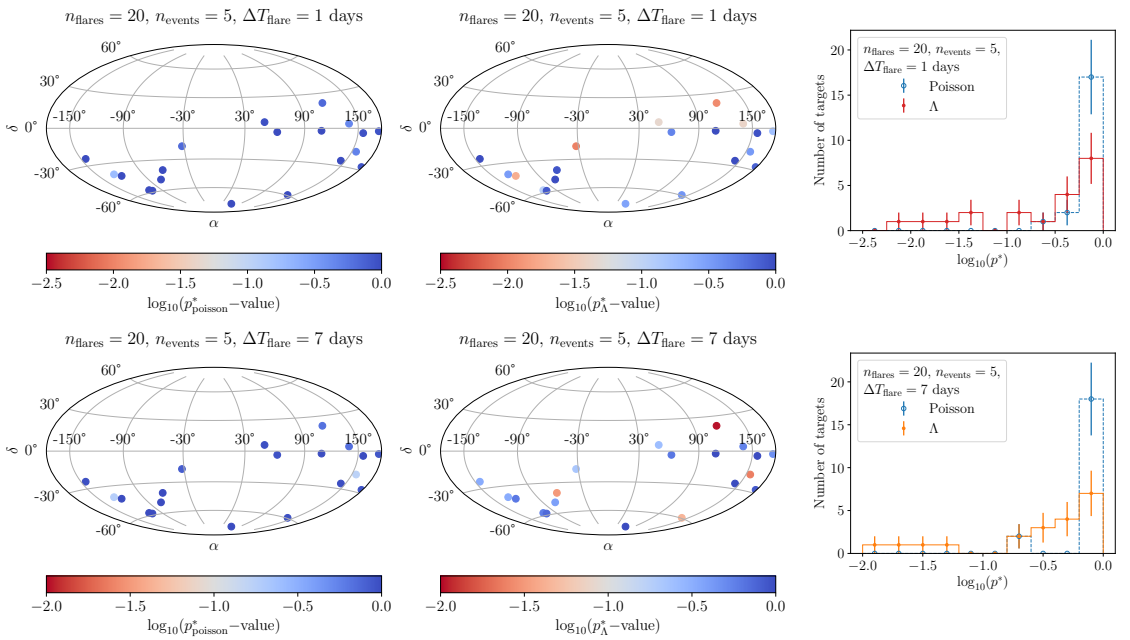

Figure 3: Upper panels: sky-maps with the penalised p-values computed from the measured number of events in each target, n (left panel) and Λ (middle panel), such that lower p-values are depicted in red and higher ones in blue, for 20 flares with 5 events each and a duration $\Delta t_{\text{flare}} = 1$ day, along with the distribution of p-values (right plot) computed from n (blue dashed) and Λ (red full). Lower panels: the same as the upper panels but for long flares with $\Delta T_{\text{flare}} = 7$ days. Its p-value distribution over the whole sky is depicted in orange in right panel.

that the significance has a dependence on the declination of the sources, although this dependence could be eliminated by weighting the p-values by the exposure. This will be done in the future.

In summary, it is evident that using Λ instead of just the integrated number of events in each target boosts the sensitivity to flares of neutral particles, both short and long flares. Therefore, Λ could be used to impose unprecedented limits on the flux from sources of ultra-high energy neutral particles or allow the detection of a source.

5. Conclusions and outlook

We have explored a novel estimator, Λ, to search for excesses of high-energy neutral particles over an isotropic background of ultra-high energy cosmic rays, using both spatial and time information arrival of cosmic ray events.

Using mockdata sets with a moderate number of flares and events per flare, over an isotropic background, we have shown that for both short and long flares, the variable Λ is more sensitive to departures from spacetime isotropy, than just the number of events in each target. We have also verified that this holds true in blind and targeted searches, by comparing the *pos-trial* and penalised p-values, respectively, for both Λ and n. Moreover, the search in time was always blind and did not contain assumptions about the light curve of the flares, besides an emission uniform in time, so correlations with the timing of the flare could boost the sensitivity of Λ even more.

Given the increased sensitivity of Λ to departures from small scale spacetime isotropy, we argue that is should be used, to either detect or place stricter upper limits on the flux of very high energy neutral particles, including photons, neutrinos and neutrons, from point sources. Regarding neutrons, this would provide a mean of improving limits on their flux at the EeV scale, as neutron showers are indistinguishable from proton showers.

Finally, the method developed in this contribution will be systematically studied.

6. Acknowledgements

The authors thank the fruitful discussions with Lorenzo Caccianiga, Danelise de Oliveira Franco, Federico Maria Mariani and Marcus Niechciol, concerning important details of the analysis.

This work has received financial support from Xunta de Galicia (CIGUS Network of Research Centers) and FCT - Fundação para a Ciência e a Tecnologia, I.P., under project CERN/FIS-PAR/0020/2021. MAM acknowledges that the project that gave rise to these results received the support of a fellowship from ”la Caixa” Foundation (ID 100010434). The fellowship code is LCF/BQ/DI21/11860033. LC wants to thank financial support from Xunta de Galicia (Centro singular de investigacion de Galicia accreditation 2019-2022), grant GI-2033-TEOFPACC and ED431F2022/15, by European Union ERDF, and by the “Maria de Maeztu” Units of Excellence program MDM-2016-0692 and the Spanish Research State Agency, grant PID2019-105544GB-I00 and program "Ramon y Cajal", Grant No. RYC2019027017-I. Ministerio de Ciencia e Innovación/Agencia Estatal de Investigación PID2019-105544GB-I00; RED2018-102661-T (RENATA); and Xunta de Galicia Consolidación 2021 GRC GI-2033ED431C-2021/22 and Consolidación 2022 ED431F-2022/15.

References

[1] The Pierre Auger Collaboration, Nucl. Instrum. Methods Phys. Res. A: Accel. Spectrom. Detect. Assoc. Equip. **798**, 172 (2015).
[2] T. Abu-Zayyad *et al.*, Nucl. Instrum. Methods Phys. Res. A: Accel. Spectrom. Detect. Assoc. Equip. **689**, 87 (2012).
[3] H. Tokuno *et al.*, Nucl. Instrum. Methods Phys. Res. A: Accel. Spectrom. Detect. Assoc. Equip. **676**, 54 (2012).
[4] The Pierre Auger Collaboration, JCAP **2023** (05), 021.
[5] R. Conceição *et al.*, JCAP **2022** (10), 086.
[6] The Pierre Auger Collaboration, JCAP **2019** (11), 004.
[7] R. Abbasi *et al.* (Telescope Array), PoS **ICRC2021**, 864 (2021).
[8] The Pierre Auger Collaboration, The Astrophysical Journal **760**, 148 (2012).
[9] The Pierre Auger Collaboration, The Astrophysical Journal Letters **789**, L34 (2014).
[10] The IceCube Collaboration, Journal of Instrumentation **12** (03), P03012.
[11] The IceCube Collaboration, The Astrophysical Journal Letters **920**, L45 (2021).
[12] D. Góra *et al.*, Astroparticle Physics **35**, 201 (2011).
[13] The Pierre Auger Collaboration, PoS **ICRC2023**, 10.22323/1.444.0246 (2023).
[14] The Pierre Auger Collaboration, The Astrophysical Journal **935**, 170 (2022).
[15] The Pierre Auger Collaboration (The Pierre Auger Collaboration), Phys. Rev. D **102**, 062005 (2020).
[16] P. Sommers, Astroparticle Physics **14**, 271 (2001).
[17] C. Bonifazi, Nuclear Physics B - Proceedings Supplements **190**, 20 (2009), proceedings of the Cosmic Ray International Seminars.
[18] H. Akima, J. ACM **17**, 589–602 (1970).
[19] K. M. Górski *et al.*, The Astrophysical Journal **622**, 759 (2005).